



PAPER • OPEN ACCESS

A software-based approach for calculating spatially resolved radiation exposure for structural radiation protection in nuclear medical imaging

To cite this article: Stefan Schwan *et al* 2022 *J. Radiol. Prot.* **42** 021531

View the [article online](#) for updates and enhancements.

You may also like

- [Features of calculation and design of pavement enduring prolonged static load](#)
A V Korochkin
- [Battery Performance Analysis Combined with Circuit Simulation and Electrochemical Calculation](#)
Akihiko Kono, Michihisa Tokito, Kosuke Sato *et al.*
- [Reliability assessment of automatic process control systems for the production of concentrates of MD1 and MD2 nanostructures in terms of providing thermal vortex enrichment](#)
A D Kolosov, S A Nebogin, V O Gorovoy *et al.*



PAPER

OPEN ACCESS



RECEIVED
2 November 2021REVISED
2 June 2022ACCEPTED FOR PUBLICATION
15 June 2022PUBLISHED
29 June 2022

Original content from
this work may be used
under the terms of the
[Creative Commons
Attribution 4.0 licence](#).

Any further distribution
of this work must
maintain attribution to
the author(s) and the title
of the work, journal
citation and DOI.



A software-based approach for calculating spatially resolved radiation exposure for structural radiation protection in nuclear medical imaging

Stefan Schwan¹ , Arbia Khezami², Janina Hohnholz¹, Christoph Lerche¹  and N Jon Shah^{1,3,4,5,*} ¹ Institute of Neuroscience and Medicine—4, Forschungszentrum Jülich GmbH, Jülich, Germany² Imaging Core Facility, Forschungszentrum Jülich GmbH, Jülich, Germany³ Institute of Neuroscience and Medicine—11, Forschungszentrum Jülich GmbH, Jülich, Germany⁴ Department of Neurology, Faculty of Medicine, RWTH Aachen University, Aachen, Germany⁵ JARA—BRAIN—Translational Medicine, RWTH Aachen University, Aachen, Germany

* Author to whom any correspondence should be addressed.

E-mail: n.j.shah@fz-juelich.de**Keywords:** structural radiation protection, annual dose, ALARA, shielding, PET

Abstract

The objective of the work described is the development of a software tool to provide the calculation routines for structural radiation protection from positron and gamma emitters, for example, ¹⁸F. The calculation of the generated local annual dose in the vicinity of these radioactive sources supports the engineering of structural measures necessary to meet regulatory guidelines. In addition to accuracy and precision, a visual and intuitive presentation of the calculation results enables fast evaluation. Finally, the calculated results are presented in a contour plot for design, evaluation, and documentation purposes. A python program was used to provide the calculation routines for structural radiation protection. For simplicity, the radiating sources can be considered as point sources. The attenuation of structural elements can be specified or, in the case of lead, calculated by virtue of its thickness. The calculated attenuation for the lead shielding is always slightly underestimated, which leads to a marginally higher calculated local dose rate than would be physically present. With the conservatively determined value, the structural radiation protection can be optimised in accordance with the general rule of as low as reasonably achievable. The pointwise comparison between the software results and the standard procedure for calculating the dose of points in space leads to similar values. In comparison with the general approach of calculating single representative points in the radiation protection area, the visual and intuitive presentation of the results supports the design and documentation of the measures required for structural radiation protection. In the present version of the software, the local dose rate and local annual dose are overestimated by a maximum of 4.5% in the case of lead shields. The proposed software, termed RadSoft, was successfully used to develop the structural radiation protection of a controlled area for hybrid magnetic resonance - positron emission tomography imaging, with the focus herein being on the requirements for PET.

1. Introduction

When implementing a controlled area in nuclear medicine, structural radiation protection is an essential part of the planning process. The aim is not only to meet legal requirements but to also ensure that the annual dose exposure for individuals is as low as reasonably achievable (ALARA) [1] and that costs are optimised through careful planning.

For Germany, the essential requirements for radiation protection for nuclear medical facilities are specified in DIN⁶ 6844 [2–4]. An additional document defines general guidelines for medical use⁷.

The current state-of-the-art for the calculation of structural radiation protection in medical imaging facilities is the assessment of representative points in workspaces, i.e. locations with a high probability of personnel being stationary with predictable residence time. In cases of multiple sources, the induced dose rate of each source is superimposed. The result is a table with the indication of sources, shielding and the calculated local dose rate for representative points in space [5].

However, this simple model does not detect hotspots in working environments caused by the superposition of radiation from multiple radioactive sources in complex building structures. Thus, sufficient important information for the assessment and optimisation of structural radiation protection is not available. To reliably detect hotspots, the local dose rate and local annual dose should be calculated for a large number of equidistant points in the entire area.

In response to this, a more comprehensive model that calculates the spatially resolved dose rate for the operating area and its surroundings is presented⁸. The approach provides more detailed insight into the extent of radiation exposure and enables a much more sophisticated optimisation of working area geometry, the location of sources, and the material and thickness of the shielding required [6].

Moreover, in the approach presented here, it is possible to define the working areas and working hours for employees and to determine the radiation times of the sources. As a result, a detailed, colour-coded plot of the annual dose for the workspaces in the radiation protection area and its surrounding area can be generated. Any hotspots that may appear are also made visible in the annual dose plot and can be assessed and mitigated if necessary. As a result, the plots provide a superior basis for interpreting the results and compiling the documentation required for structural radiation protection. In comparison to programs with complex 3D simulations such as Microshield⁹, the focus of the tool presented here is on the spatial representation of the local dose rate and local annual dose, calculated in accordance with the methods used in structural radiation protection for medical nuclear imaging. 3D simulation tools would be far too complex for this purpose as the creation of the model would be too time-consuming and the evaluation far too convoluted. To the best of our knowledge, a software tool that supports structural radiation protection planning in the manner described is not currently widely available.

The proposed software has been used, by way of example, for calculating the dimensions of the radiation protection of an magnetic resonance - positron emission tomography (MR-PET) imaging facility, but its applicability goes beyond the specified use illustrated here. In general, the concept can be applied to the design of the structural radiation protection for any type of point-like sources in accordance with the conditions described below.

2. Concepts

Structural radiation protection is based on fixed building structures and permanently installed shields to reduce the local dose rate in rooms with workspaces adjacent to a source but not in the room containing the source. Hence, the distances between a source and the employees are normally relatively large. Thus, the inhomogeneity of the radiation on a person is negligible for the calculation of structural radiation protection measurements. Consider a point source placed 85 cm above floor level (e.g. on a table) whose radiation intensity decreases with the inverse square of the distance, the partial body radiation differs for a 1.7 m tall person by 8% at a distance of 3 m and by 2% at a distance of 6 m¹⁰. Accordingly, extended sources are processed like point sources. Taking this assumption into account, the dose rate, \dot{H}_0 in mSv h⁻¹, can be calculated by the inverse square law using equation (1), where d is the distance (in meters) between the source and a point in space at position x, y on a grid where the exposure would be caused. Γ is the nuclide specific dose rate constant (in mSv m² h⁻¹ GBq⁻¹), and A is the activity of the source (in GBq). The calculation assumes a point-like source of gamma radiation without consideration of any shielding [7]:

$$\dot{H}_0(x, y) = \frac{\Gamma \cdot A}{d^2}. \quad (1)$$

By way of example, table 1 shows the dose rate constants of some commonly used PET nuclides [8]. The constant is nuclide specific and converts the activity into the dose rate. With its introduction, the radiological

⁶ DIN: German Institute for Standardisation.

⁷ Bundesamt für Strahlenschutz: Strahlenschutz in der Medizin—Richtlinie zur Strahlenschutzverordnung (StrlSchV).

⁸ RS Designer software: www.511kev.com/rs-designer.

⁹ Microshield: <https://radiationsoftware.com/microshield>.

¹⁰ Difference in radiation intensity at the head or feet compared with the centre.

Table 1. Dose rate constants of common PET nuclides [8].

Nuclide	Γ (mSv m ² h ⁻¹ GBq ⁻¹)
¹¹ C	0.1707
¹³ N	0.1707
¹⁵ O	0.1709
¹⁸ F	0.1655
⁶⁸ Ge	0.158
²² Na	0.3344
¹³⁷ Cs	0.0927

effect of different nuclides may be compared. If the distance between a source and an employee in an adjacent room is not sufficient to adequately limit the local dose rate, partition walls made of special construction materials, such as barite concrete, can be used as shielding. Furthermore, additional lead panels can be added to structural components. A shield reduces the local dose rate, \dot{H}_0 , by a factor given by the attenuation, F , resulting in the absolute dose rate, \dot{H} , of a grid point (equation (2)). The achieved attenuation factor, F , depends on the material of the shield itself, the thickness of the material and the energy spectrum of the radiating nuclide. The angle at which the radiation penetrates the shield, and thus the path length of the radiation through the shield, is not considered in the approach presented here. This assumption leads to an overestimation of the local dose rate computed by using the shortest perpendicular path through the medium and therefore leads to a conservative dose estimate:

$$\dot{H}(x,y) = \frac{\dot{H}_0(x,y)}{F}. \quad (2)$$

In the dataset of the software, the attenuation F , can be specified for each constructive element. In the case of gamma photons from ¹⁸F, the software calculates the attenuation from a given thickness, t , of a lead shield (equation (3)):

$$F = \begin{cases} 0.975 \cdot e^{0.136 \cdot t}, & \text{for } 1 \text{ mm} < t \leq 13 \text{ mm} \\ 0.8128 \cdot e^{0.15 \cdot t}, & \text{for } 13 \text{ mm} < t \leq 42 \text{ mm} \\ 0.6517 \cdot e^{0.1553 \cdot t}, & \text{for } 42 \text{ mm} < t \leq 100 \text{ mm} \end{cases}. \quad (3)$$

The functions are determined by the published data from NAR¹¹. The parameters are set in such a way that the attenuation of the shielding is underestimated by up to 4.5% in the case of lead shields. Thus, the absolute dose rate, \dot{H} , is always overestimated, leading to a safe approach. In a first approximation, the attenuation depends on the Beer–Lambert law and thus on an exponential function. However, for lead thicknesses from 1 to 100 mm, the attenuation is also influenced by scattering, for example, within the small, specified intervals, the given data by NAR can be approximated by an exponential function with sufficient accuracy.

If there are n shields between a source and a grid point, the attenuation factors, F_n , of the shields are multiplied to determine a representative single value F_{total} :

$$F_{\text{total}} = F_1 \cdot F_2 \cdot F_3 \cdot \dots \cdot F_{n-1} \cdot F_n. \quad (4)$$

With the above formulas, the local dose rate of one source can be evaluated for each grid point.

Usually, various discrete sources are handled in a controlled area. In a worst-case scenario, the sources radiate simultaneously. Hence, the single local radioactive dose rate $\dot{H}(i)$ of every source is superimposed to a total local radioactive dose rate \dot{H}_{total} of all sources for every grid point:

$$\dot{H}_{\text{total}}(x,y) = \sum_{i=1}^{i=n} \dot{H}(i,x,y). \quad (5)$$

When calculating the dimensions of shields, the local dose rate of the room where the source is located is conventionally not considered in structural radiation protection. Thus, the local dose rate of the source in the room containing the source is set to zero. Protection against the radiation of local sources comes under the remit of the radiation protection instruction of the facility and is subject to the introduction of local

¹¹ DIN-Normenausschuss Radiologie (NAR); www.din.de/de/mitwirken/normenausschuesse/nar/berechnung-von-abschirmdicken-fuer-die-nuklearmedizin-79934.

measures. Local measures are, for example, local shields in the workspaces, increased distance to the source and short residence times of the staff.

Finally, the annual exposure time for each area must be specified in order to assess the radiation protection of the staff. A workspace is defined as an area in a room that is freely accessible by the staff, i.e. areas containing fixed structures that limit the dimension of the workspace are excluded. In this context, workspaces with estimated working hours can be defined. To determine the local annual dose, H , working hours t_w for each workspace and the irradiation time t_s of every source must be considered. The exposure time is shorter of the two, the working hours and the irradiation time. Conservatively, it is assumed that the working hours and the irradiation time always overlap. Minimum values for the irradiation time and the working time in workspaces and corridors are specified in the standard DIN6844-3 [3]. The annual dose, $H(i)$, for a worker at any of the points in a workspace is calculated according to:

$$H(x, y) = \begin{cases} \dot{H}(x, y) \cdot t_w, & \text{for } t_s > t_w \\ \dot{H}(x, y) \cdot t_s, & \text{for } t_s \leq t_w \end{cases} \quad (6)$$

The total local yearly dose, H_{total} , can be superimposed for every point in a workspace with the following equation:

$$H_{\text{total}}(x, y) = \sum_{i=1}^{i=n} H(i, x, y). \quad (7)$$

The computational result is a local annual dose plot, which is essential for the assessment of constructive radiation protection measures. By estimating the annual dose of a workspace, the dose to the employee can be estimated, and thus the radiation protection area can be assessed. The radioactive decay of the source is not considered in the calculation. If the average radioactivity, \bar{A} , of the source needs to be considered, it can be calculated with equation (8), where $T_{1/2}$ is the half-life and t_s is the irradiation time:

$$\bar{A} = A_0 \cdot \frac{T_{1/2}}{t_s \cdot \ln(2)} \left(1 - e^{-\frac{t_s \cdot \ln(2)}{T_{1/2}}} \right). \quad (8)$$

3. Software concept

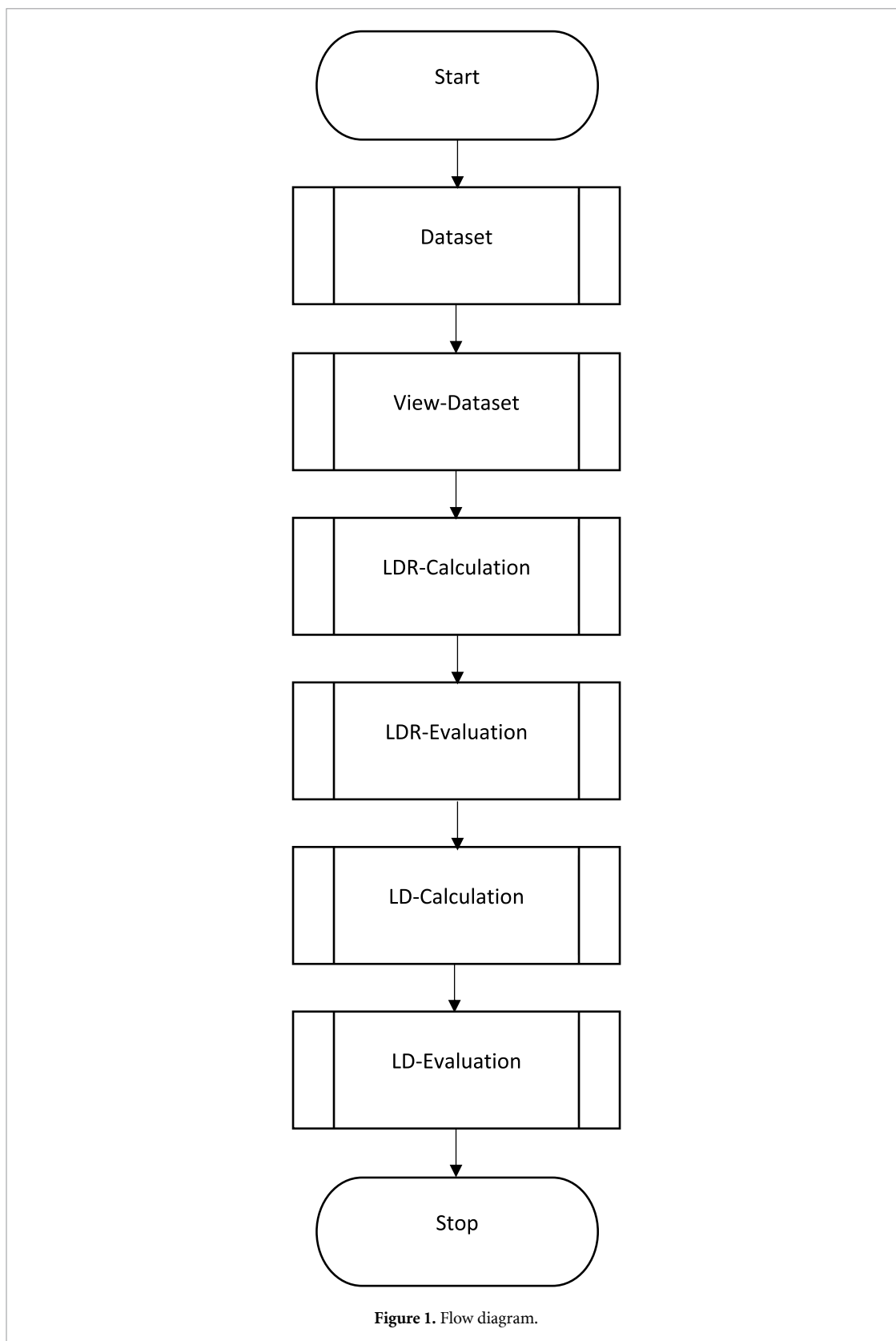
The RadSoft software package presented here contains the calculation routines in six separate applications coded in Spyder¹². The focus of this work is to create a simple software solution covering the method described above. Because of the absence of a graphical user interface, all structures in the building must be defined by textual input. Figure 1 shows the flow chart of the applications described below. Each application can be started as an independent routine using the data generated by the previous routine. The software is available upon request and may be used in the framework of scientific collaborations, whereby the recipient organisation assumes full legal responsibility for the use of the software.

To begin with, the subprogram *DATASET* defines building structures, sources, and shields. Markers, displayed as yellow crosses, are then defined to readout the calculated radiological values of a grid point. Additionally, the spatial model size and spatial resolution are defined. Initial calculations can then be carried out by choosing a low resolution to get an initial impression of the data and existing radiation protection measures. The maximum digitising error corresponds to the chosen grid resolution, res , and the distance, d , between the source and a grid point. The error decreases by increasing the distance between the source and the grid point. With a suitable resolution of a few centimetres, the digitisation error is negligible, as the distance between the source and the grid point to be assessed is generally a few metres. Equation (9) gives the maximal digitising error, E , of the dose rate, \dot{H}_0 , where d is the distance between the source and the grid point and res is the resolution specified for conducting the calculation:

$$E = \left(1 - \left(\frac{d}{d + \sqrt{2} \cdot \text{res}} \right)^2 \right) \cdot 100\%. \quad (9)$$

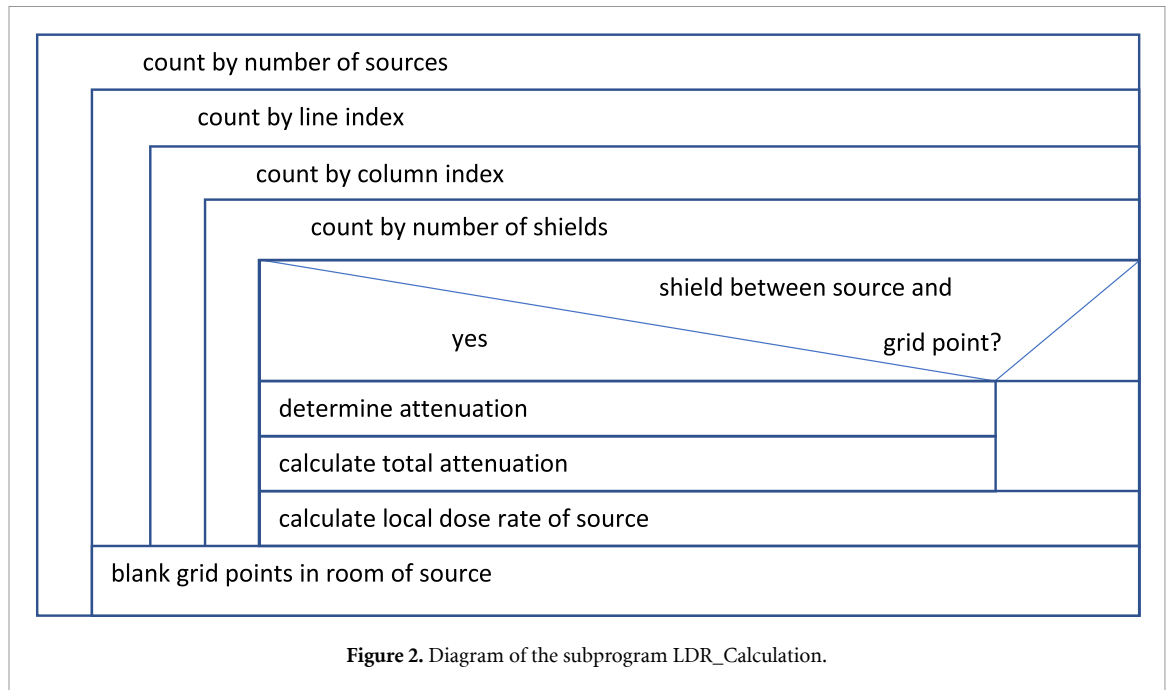
Building structures with no relevant shielding effect, i.e. stud walls without added shielding, are specified as lines and are displayed in yellow. They are only added for orientation and do not affect the results. Shields are displayed as red lines and are defined by their geometrical specifications and their attenuation.

¹² Spyder: Scientific Python Development Environment.



The attenuation coefficient of common building materials can be obtained using reference tables¹³. In the case of lead shields, the software calculates the attenuation based on the thickness of the lead.

¹³ DIN-Normenausschuss Radiologie (NAR); www.din.de/de/mitwirken/normenausschuesse/nar/berechnung-von-abschirmdicken-fuer-die-nuklearmedizin-79934.



The sources are defined by their location, activity, irradiation time, and the dimension of the room in which they are located. The dimensions of the room define the area around a source, which is set to zero in the calculation routine. Finally, workspaces, displayed as cyan squares, are specified by their dimensions along with the indicated working hours. In general, sources are modelled as a point source and shields as a one-dimensional line.

Before calculating, the dataset can be reviewed with the subprogram *VIEW_DATASET*.

With the specified dataset, the subprogram *LDR_CALCULATION* calculates the local dose rate for all sources. The calculated data of each source are stored in a separate matrix representing the grid. The programme follows the approach described in the previous section. Figure 2 shows a very rough overview of the algorithm. The outer loop starts the spatially resolved calculation of the local dose rate for each source. The next two loops run sequentially through the array elements. Each element corresponds to a grid point storing the local dose rate. A query is then used to check whether a shield crosses the path of the gamma ray between the selected source and the grid point. The total attenuation factor is calculated for all shields between the source and the grid point. The local dose rate is calculated based on the determined data. The local dose rate of the source in its room is ignored.

Subsequently, the local dose rate can be displayed with the subprogram *LDR_EVALUATION* for all or selected sources. Displaying the spatial dose rate of selected sources is required for adjusting measures in structural radiation protection, such as the inclusion of additional shields, and for identifying the optimal positioning of shields or sources.

The subroutine *LD_CALCULATION* is now used to calculate the local annual dose for each workspace-source combination. Figure 3 shows a very rough overview of the algorithm. First, the exposure time is determined by calculating the minimum radiation time of the source and the time the employees remain in the workspace. The local annual dose is then calculated for each point of the workspace using the local dose rate and the exposure time.

Finally, the local annual dose can be displayed with the subprogram *LD_EVALUATION* for all or selected sources. The local annual dose at the marker positions is displayed by the software in a table.

4. Example computation

Figure 4 shows the arrangement of sources and shields chosen for an example evaluation. A T-shaped shield constructed from 5 mm thick lead separates rooms A, B, and C from each other. Additionally, a further shield of 5 mm thick lead is located at the back of room A.

A resolution of 2.5 cm was chosen for the calculation. To avoid digitisation errors, the position of all sources and markers was an integer multiple of the grid resolution.

First, the local dose rate of source S1, with a radioactivity of 250 MBq ^{18}F , in room B was investigated. Based on this calculation, a second source, S2, that is mirror-symmetric to source S1 and of the same

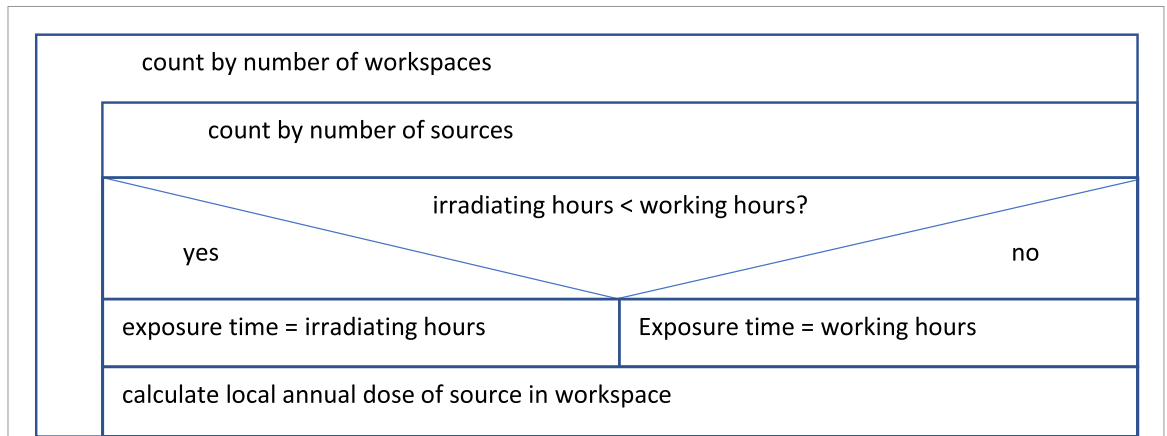


Figure 3. Diagram of the sub-program LD_Calculation.

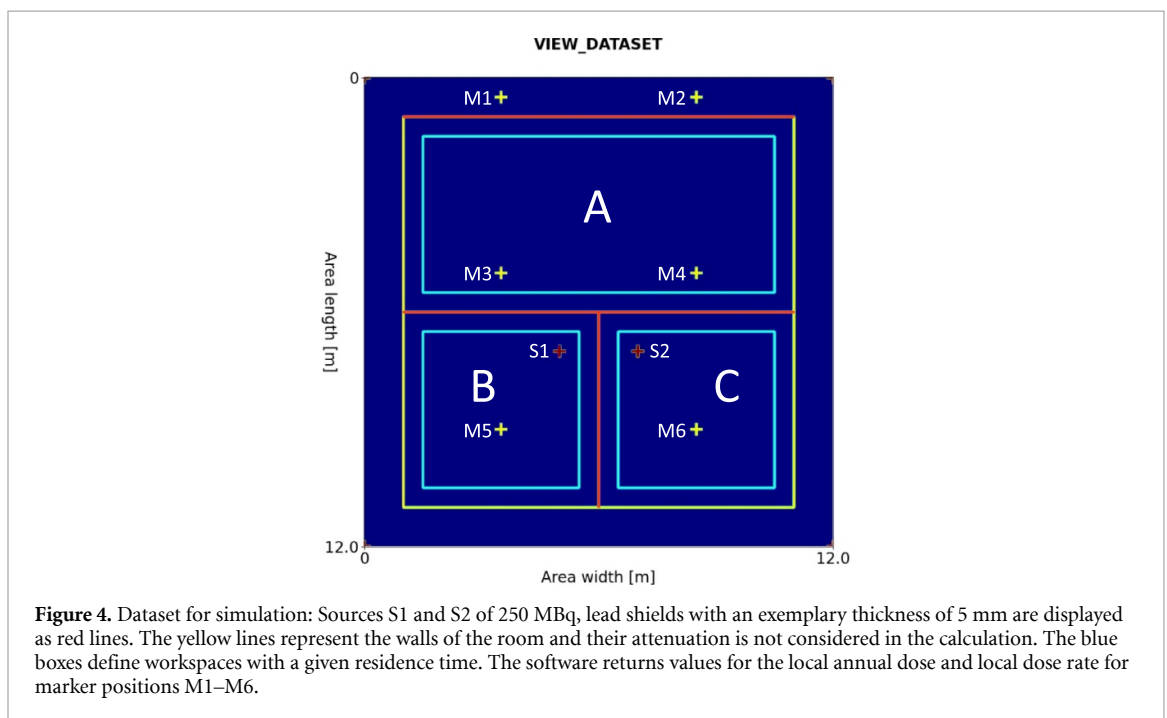


Figure 4. Dataset for simulation: Sources S1 and S2 of 250 MBq, lead shields with an exemplary thickness of 5 mm are displayed as red lines. The yellow lines represent the walls of the room and their attenuation is not considered in the calculation. The blue boxes define workspaces with a given residence time. The software returns values for the local annual dose and local dose rate for marker positions M1–M6.

radioactivity, was introduced in room C. As a proof of concept, the calculation of the local dose rate for the single source, S1, and the mirror-symmetric sources, S1 and S2, was carried out both with and without considering the fraction of radiation generated inside the room where the source was located. The arrangement provides intuitive access to the workflow and the output of the software. When one considers a mirror-symmetric arrangement, the superposition of the radiation of multiple sources causes a mirror-symmetric local dose rate distribution.

Subsequently, the annual dose was calculated and is displayed for the defined workspaces in rooms A, B, and C. The evaluation was carried out for both sources and with and without considering the radiation from the source inside the room itself. The exposure time of each workplace was considered to be 4 h per day, resulting in an annual working time in the presence of a source of 1000 h per year. By assuming a uniform exposure time, the result remains mirror-symmetric and can be directly compared with the result of the local dose rate.

Finally, the numerical output of the markers M1 to M6 was verified to check the calculation results of the software. As the dose rate distribution of a mirror-symmetric task has a mirror-symmetric result, the markers are placed in a mirror-symmetric way. Thus, it is sufficient to evaluate the numerical values of the markers M1, M3, M5 and to compare the results with the respective mirror-symmetrical markers M2, M4, M6. Further values can be retraced in the contour plots.

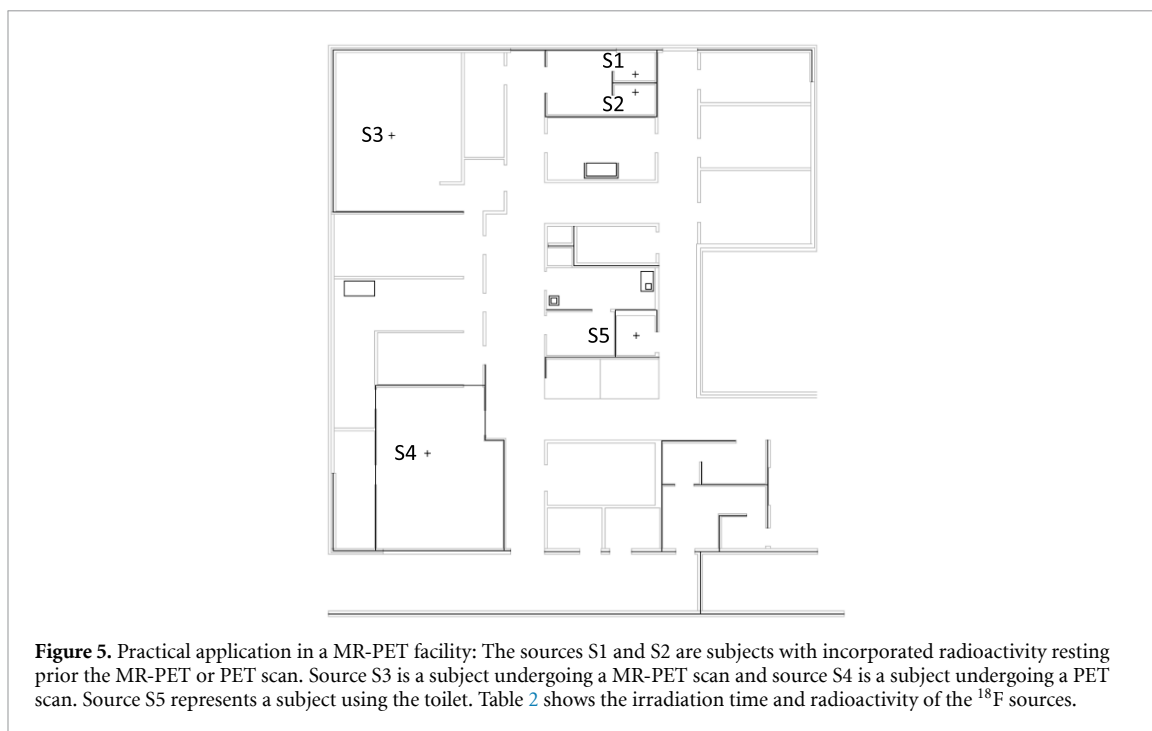


Figure 5. Practical application in a MR-PET facility: The sources S1 and S2 are subjects with incorporated radioactivity resting prior the MR-PET or PET scan. Source S3 is a subject undergoing a MR-PET scan and source S4 is a subject undergoing a PET scan. Source S5 represents a subject using the toilet. Table 2 shows the irradiation time and radioactivity of the ^{18}F sources.

Table 2. Definition of the sources in the practical application. The irradiation nuclide is ^{18}F .

Source	Irradiation time (h d^{-1})	Radioactivity (MBq)
S1	5	308
S2	5	308
S3	7.5	208
S4	7.5	258
S5	1.24	212

Table 3. Attenuation of concrete walls next to a source.

Position of concrete walls (see figure 6)	Attenuation
A	10.6
A1	3.9
A2	21.6

5. Practical application

The example application considers radiation protection in an area used for MR-PET and PET measurements. Figure 5 shows the location, and table 2 shows the radioactivity as well as the irradiation time of the sources. The exemplary values for the source activity are mean values obtained by averaging over the irradiation time of the source, i.e. the patient with injected activity, assuming the half-life of ^{18}F . Sources S1 and S2 are subjects in the resting phase before investigation. The sources are considered to radiate for 8 h per day. Subjects already undergoing examination at the MR-PET scanner are represented by S3, and subjects undergoing examination at the PET scanner are represented by S4. Depending on the subject and the kind of investigation, a radiopharmaceutical with a radioactivity of between 250 and 370 MBq is injected. Source five, with an annual radiation time of about 300 h, represents a subject using the toilet. Further sources are well shielded and are not considered in this section. In the example, a total of 8 h per day is chosen to reflect the working time in the workspaces and 200 h per year spent in the corridors. Generally, the applied time periods correspond to the standard values of the norm DIN6844-3 [3]. In the practical application, additional lead shielding was applied to the inner partition walls. The attenuations of the concrete walls next to the sources are given in table 3, and the thicknesses of the applied lead shielding are given in table 4. Figure 6 shows the position of the concrete walls and the lead shielding.

Table 4. Applied lead shielding in the partition walls.

Position of lead shielding (see figure 6)	Thickness (mm)
1	12
2	12
3	2
4	12
5	12
6	12
8	12
9	12
10	2
11	2
12	2
13	2
14	5
15	5
16	22
17	20
18	15
19	20
20	25
21	20
22	20

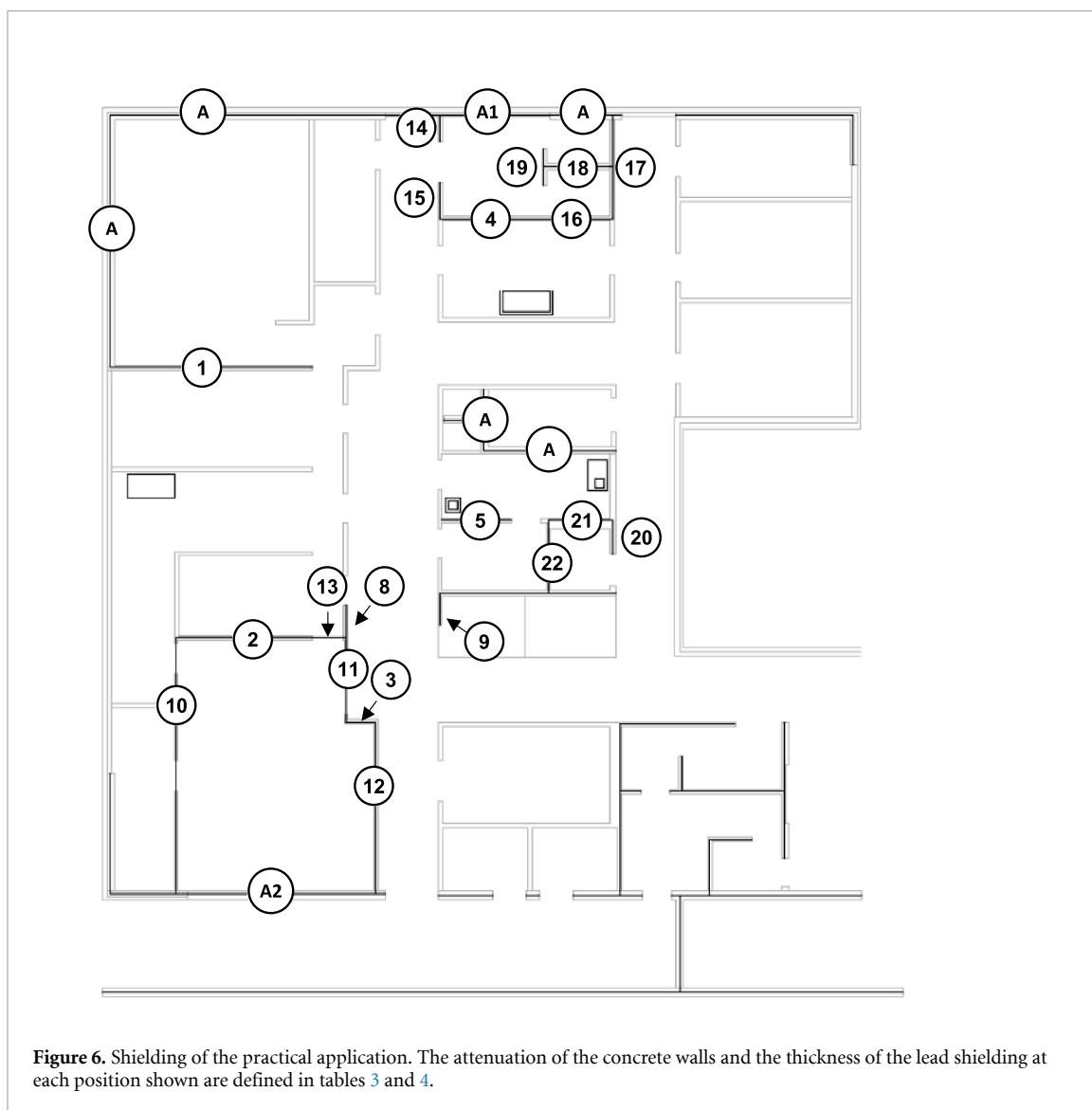
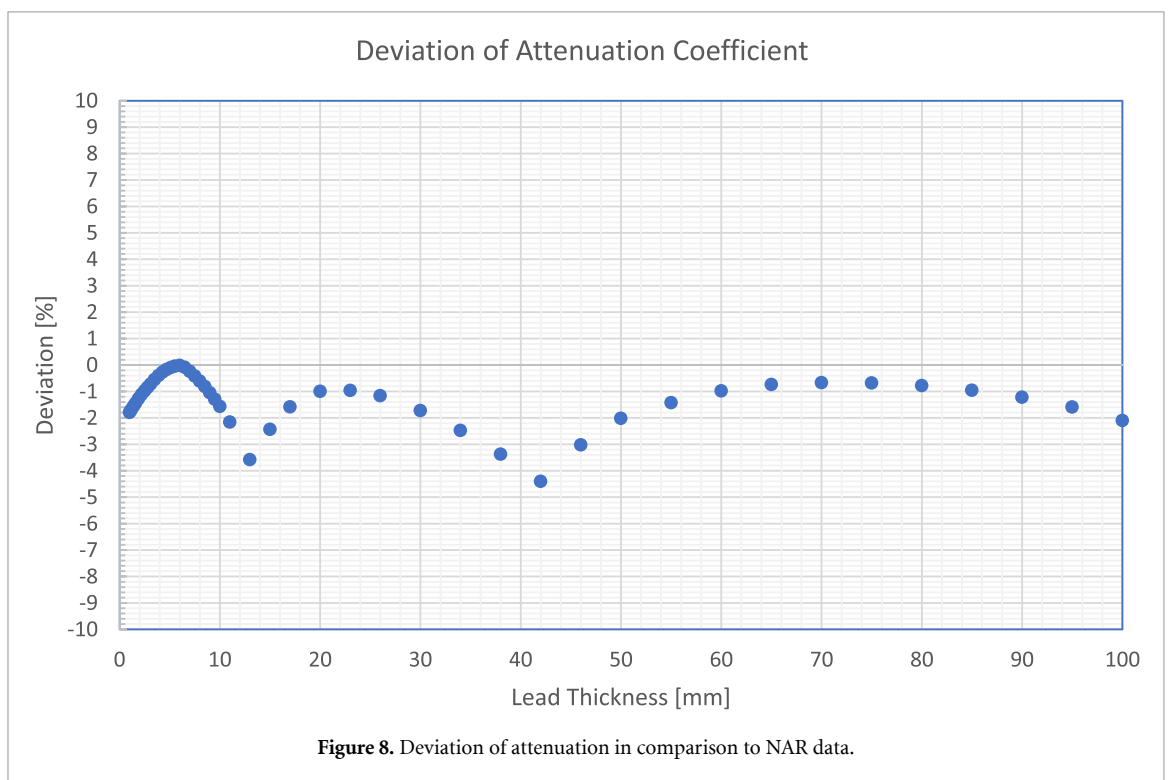
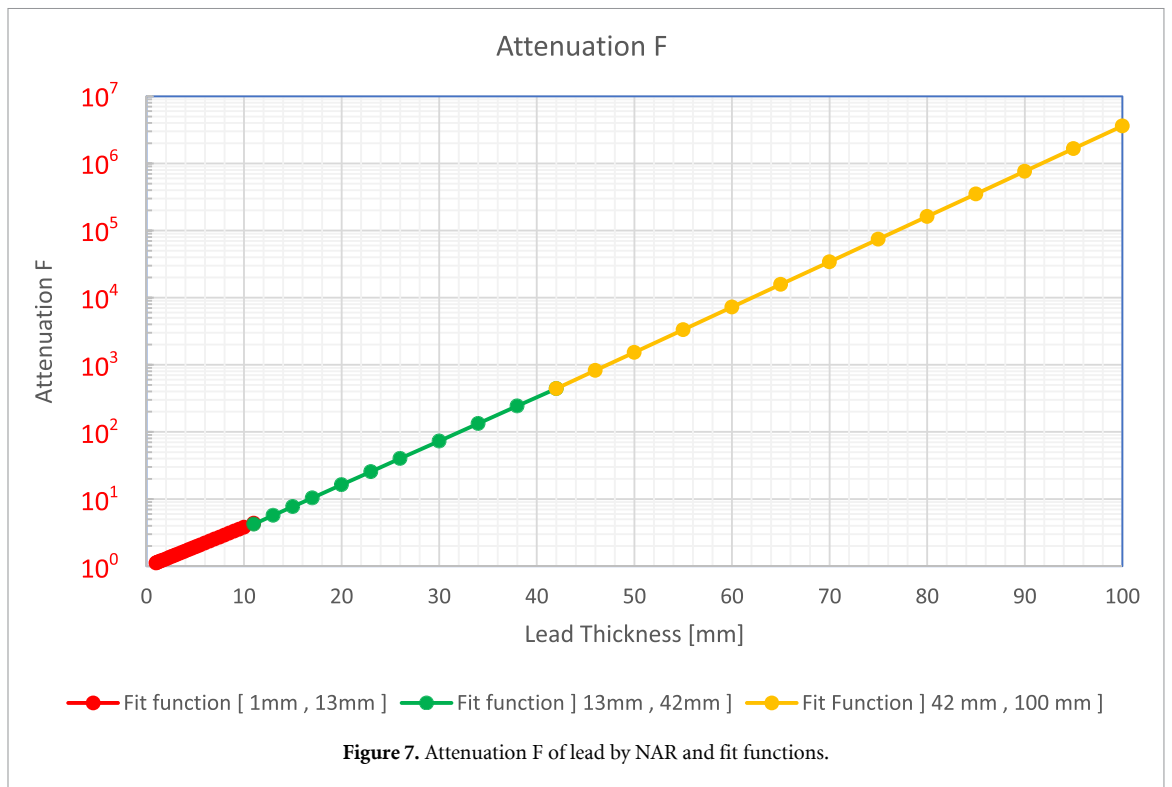


Figure 6. Shielding of the practical application. The attenuation of the concrete walls and the thickness of the lead shielding at each position shown are defined in tables 3 and 4.



6. Results

The numerical results of equation (3) are shown in figure 7. In the logarithmic diagram, the points of support from NAR are not distinguishable from the fitting function and are therefore not plotted. In comparison to the data from NAR, the attenuation factor calculated by the function deviates by a maximum of 4.5% for lead shielding and is always underestimated (figure 8).

Figure 9 shows the contour plot of the local dose rate for source S1 in room B. At a distance of 2.5 m to the source, the local dose rate is about $6.5 \mu\text{Sv}\cdot\text{h}^{-1}$, which corresponds to the yellow-coloured grid elements in the contour plot. The threshold of the plot is set to $10 \mu\text{Sv}\cdot\text{h}^{-1}$, leading to a saturation effect in the vicinity of the

source, which is displayed in dark red without any contour. When ^{18}F radiation is assumed, the lead shields with a thickness of 5 mm correspond to one half-value layer of lead for 511 keV gammas. Thus, following the yellow section from room B to room A or C, the colour of the grid elements on a circle of 2.5 m turns from yellow to light blue, which corresponds to a local dose rate of about $3.25 \mu\text{Sv h}^{-1}$. The circular radiation propagation in rooms A and C is caused by the model as the angle-dependent path length through the shield is not considered. Transmission through two shields gives rise to the dark blue sector, A1, in room A.

Figure 10 shows the local dose rate distribution of source S1, in rooms A and C, while the radiation in room B is not considered. Since there are no other sources in the other rooms, the local dose rate in room B is zero.

The spatial local dose rate distribution of the sources S1 and S2 is shown in figure 11. In room A, the local dose rate of source S1 is superimposed by the radiation of source S2, which is shielded with one half-value layer of lead for 511 keV. Room C shows the mirror-symmetrical dose rate distribution of room B. The T-shaped shielding forms the three sectors, A2, A3 and A4, each containing a different dose rate distribution. Sector A2 shows the superimposed dose rate of source S1, shielded with one half-value layer of lead, and source S2, shielded with two half-value layers of lead. Sector A4 shows the mirror-symmetrical dose rate distribution of sector A2. The dose rate of sector A3 is superimposed by the radiation of sources S1 and S2, both shielded with only one half-value layer of lead.

Figure 12 shows the local dose rate distribution of the sources S1 and S2 with the radiation source in the room not considered. The local dose rate in room A does not change. Room B shows the local dose rate of source S2 shielded by one half-layer of lead; conversely, room C only shows the resulting local dose rate of source S1 shielded by one half-layer of lead.

Figure 13 shows the calculation results of the local annual dose for the workspaces. The colour of the contour plot inside the workspaces corresponds to figure 11 due to the chosen annual exposure time of 1000 h. Outside the workspaces, the exposure time, and thus the dose, is zero.

Finally, the radiation of the source within its room is neglected. The resulting local annual dose is shown in figure 14. In accordance with the chosen parameters, the colour coding of the local annual dose within the workspaces corresponds to the colour coding of the local dose rate in figure 12.

Table 5 shows the numerical results for the marker positions M1 to M6. The calculated values correspond to the output values of the software and the colour coding of the figures. For reasons of symmetry, the numerical values of the dose rates and doses of the markers M1, M2, as well as M3, M4 and M5, M6 are equal.

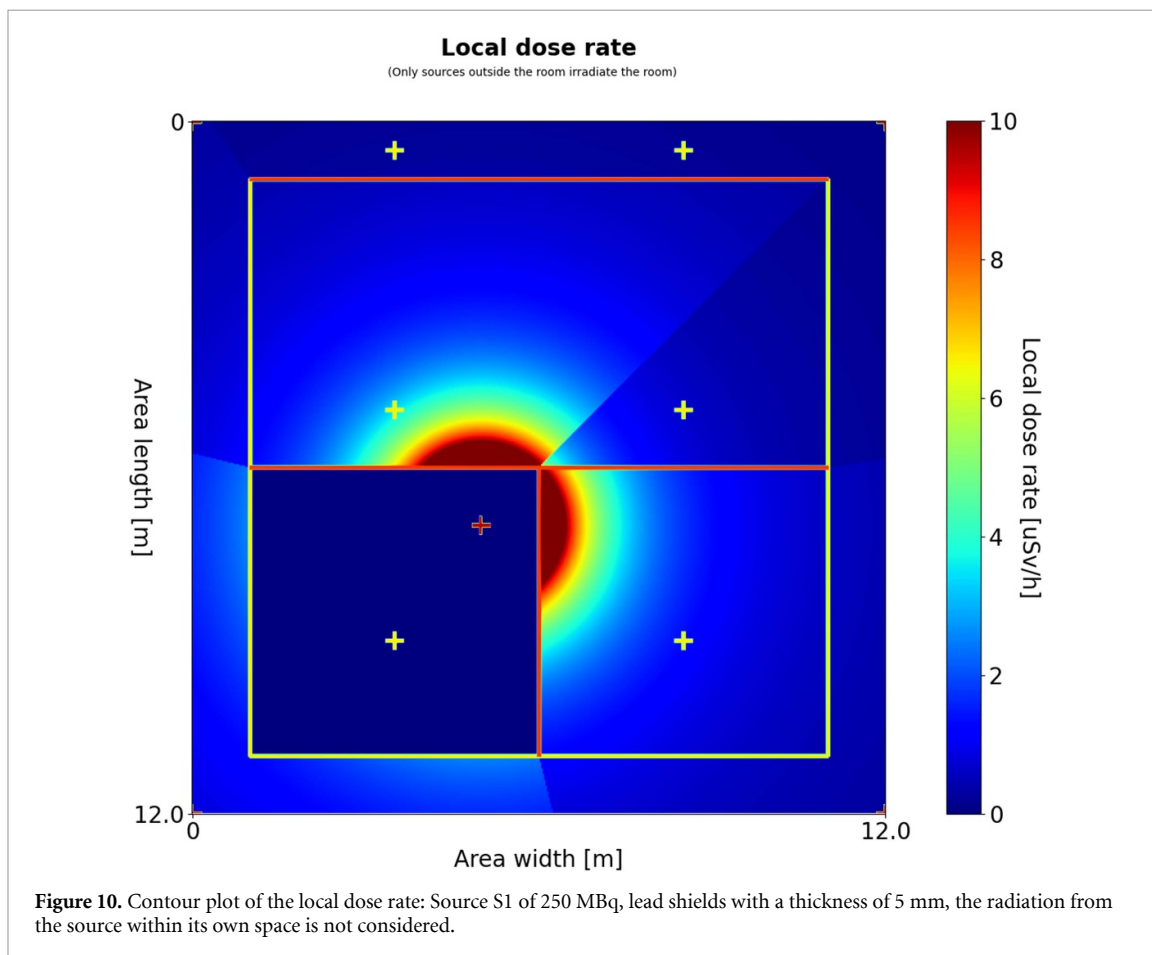
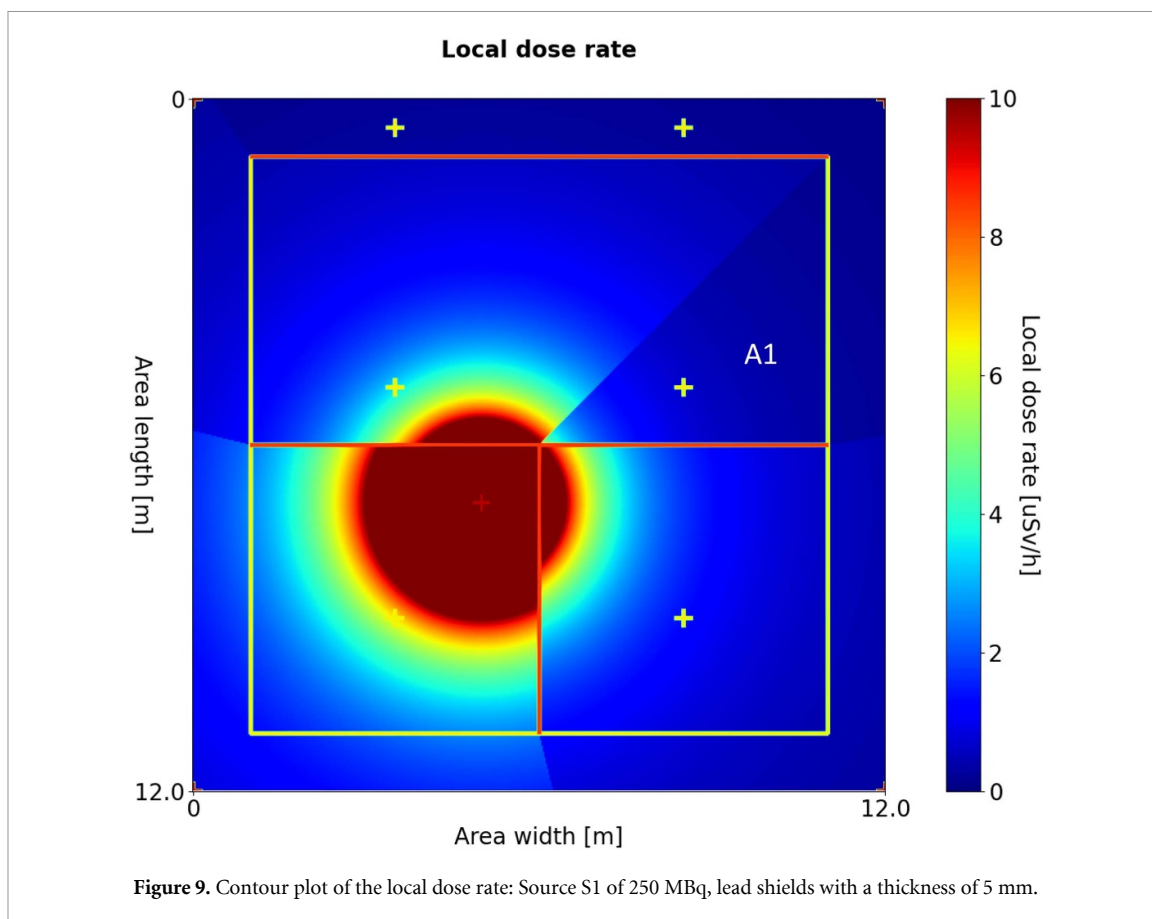
Figures 15–18 show the results of the radiation protection calculation for an MR-PET facility. Figure 15 shows the contour plot of the local dose rate. The radiation paths of individual sources and the superposition of the local dose rates are clearly visible. The superposition is obvious, for example, in the corridor to the right of sources S1 and S2. Within rooms containing a radiation source, the radiation of the source is the dominant contribution to the radiation in the respective room. Irradiation from sources outside the room adds almost no contribution. Figure 16 shows the contour plot of the local dose rate when the radiation from the source within its own space is omitted. Thus, only the irradiation from outside the room into this room is considered. The local dose rate is low, and therefore the room appears blue, as blue corresponds to low dose rates. The contour plot of the local annual dose is shown in figure 17. High doses correspond to the red areas in the contour plot and can be seen in the immediate vicinity of a radiation source. However, figure 18 shows the impact of the structural radiation protection measures. When calculating the annual dose, only the local dose rate irradiated into the room and the determined exposure times are considered.

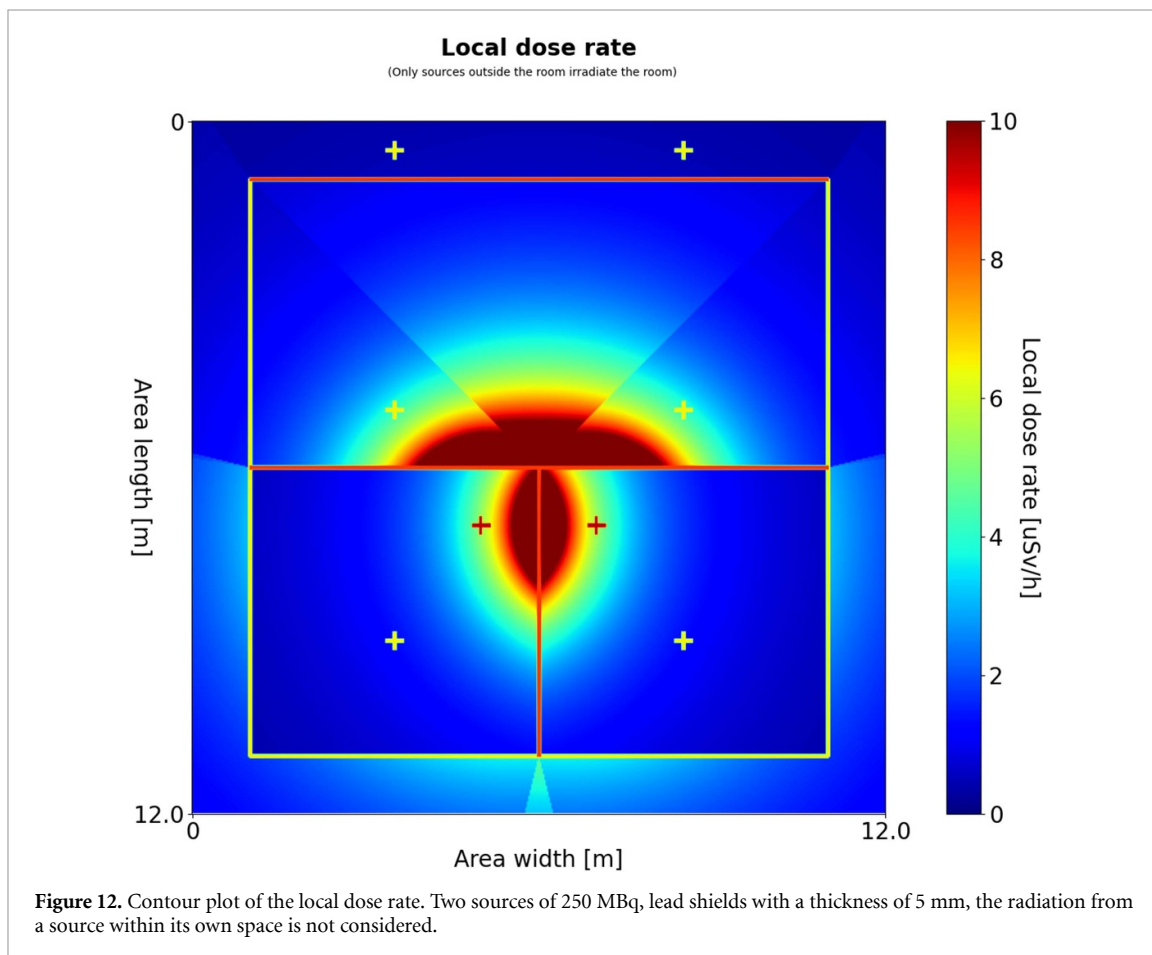
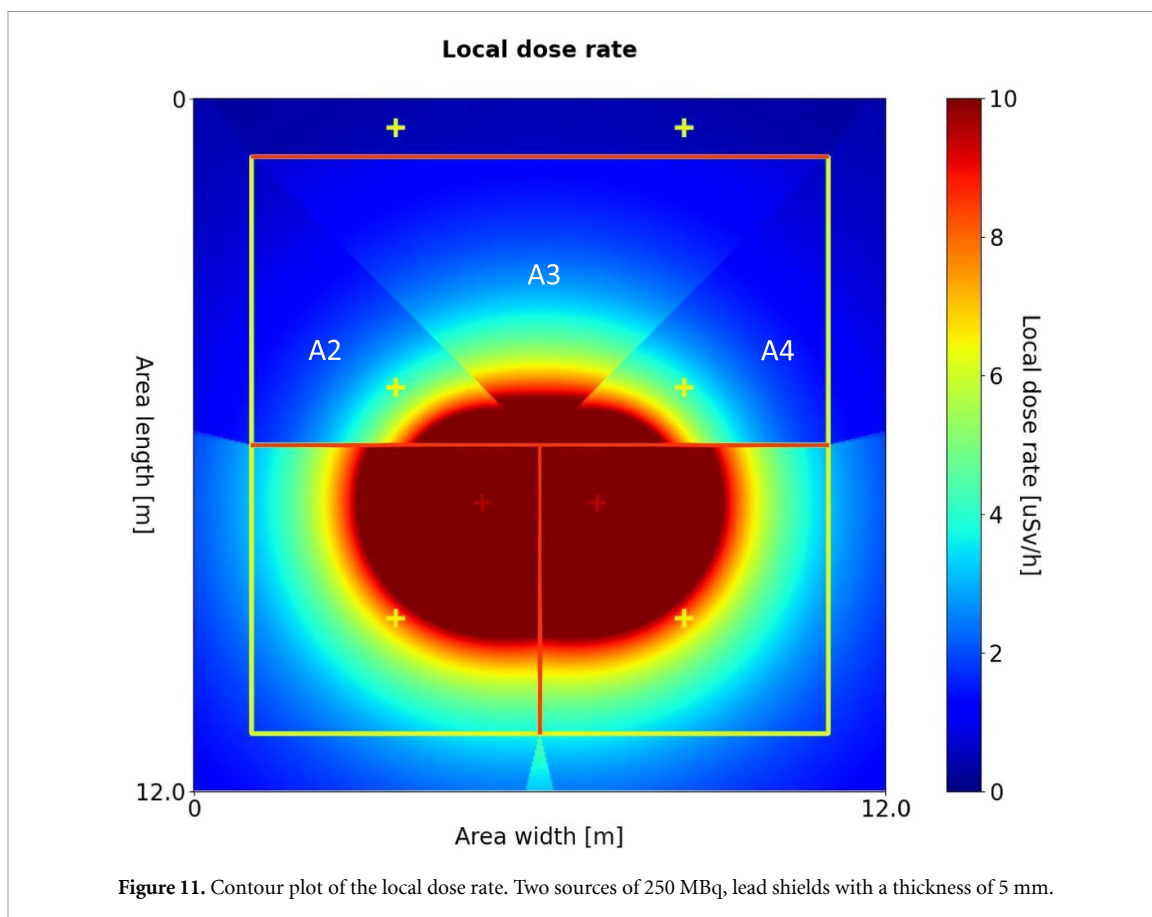
7. Discussion

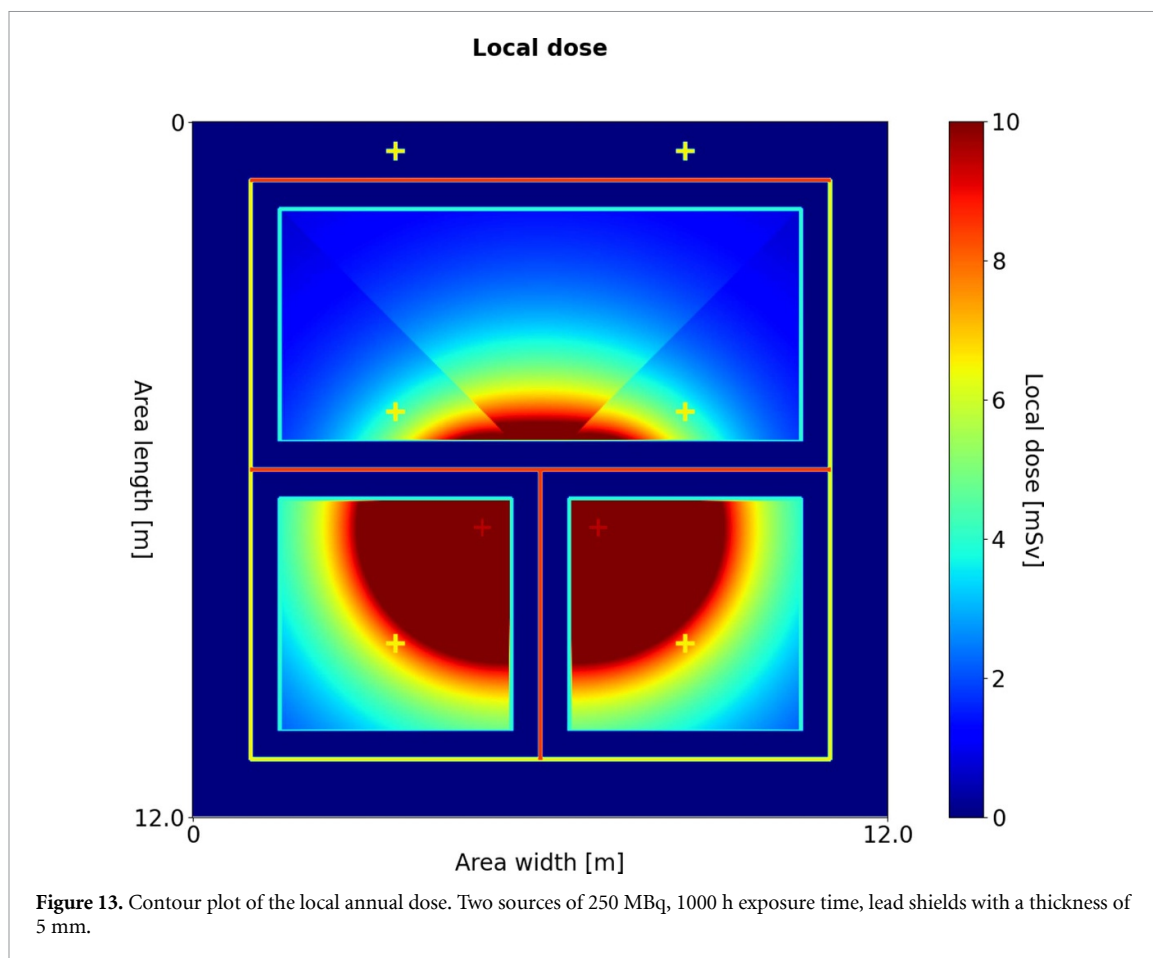
The calculated attenuation of the lead shielding is up to 4.5% lower than the attenuation for lead shields published by NAR. Hence, the local dose rate is overestimated, which always keeps the calculation conservative. The attenuation for all other constructive measures is directly defined by the user in the dataset.

Table 5 shows the conventional calculation method for the design of structural radiation protection. At the same time, the data are used to benchmark and validate the software results. The advantage of the visual presentation of the results in contour plots is that markers can be positioned on hotspots in the working areas. Thus, the structural radiation protection can be optimised according to the selected maximum dose values. An underestimation of the dose can therefore be ruled out in practice. Accordingly, the dose rate contour plots and the annual dose calculation enable simple yet precise structural radiation protection planning. For example, the contour plot for sector A3 shown in figure 11 clearly highlights a hotspot created as a result of sources S1 and S2, thus enabling structural measures to be put in place as part of the planning process.

In the example shown in figure 4, the hotspots can be identified by an experienced radiation protection adviser using the conventional approach of calculating the local dose rate and local annual dose for selected







points in space. However, in a more complex assembly with a variety of sources, such hotspots can only be identified with a spatially resolved contour plot, as generated by the proposed software package. These spatially resolved dose rate plots and dose plots enable a reliable assessment of workspaces, and weak points in the structural radiation protection concept can be easily recognised and eliminated in a systematic manner. The ability to jointly consider both the spatially resolved local dose rate and the local annual dose is particularly advantageous as, in contrast to the local annual dose, the local dose rate is not weighted by exposure time. This makes hotspots in the contour diagram of the local dose rate more visible and easier to investigate, and, moreover, measures to eliminate the increased dose rate are now simple to model and evaluate for effectiveness. In addition to these factors, the contour diagram can be used to determine whether an increased local dose rate leads to an increase in the local annual dose above the legal limit. However, the local annual dose must be ALARA. The presentation of the local annual dose in contour plots is sufficient for the verification of structural radiation protection according to the DIN 6844 standard. It can supplement the tabular representation of values in the documentation.

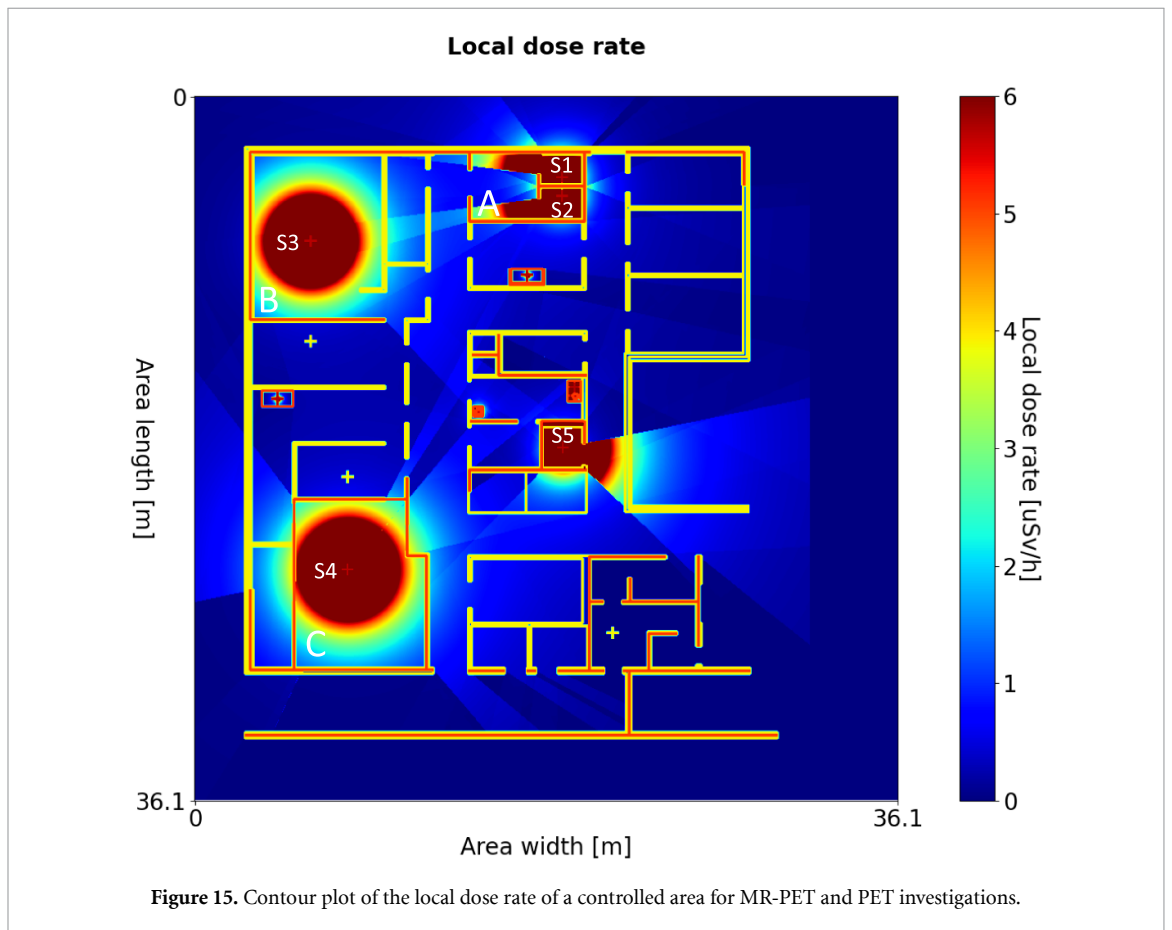
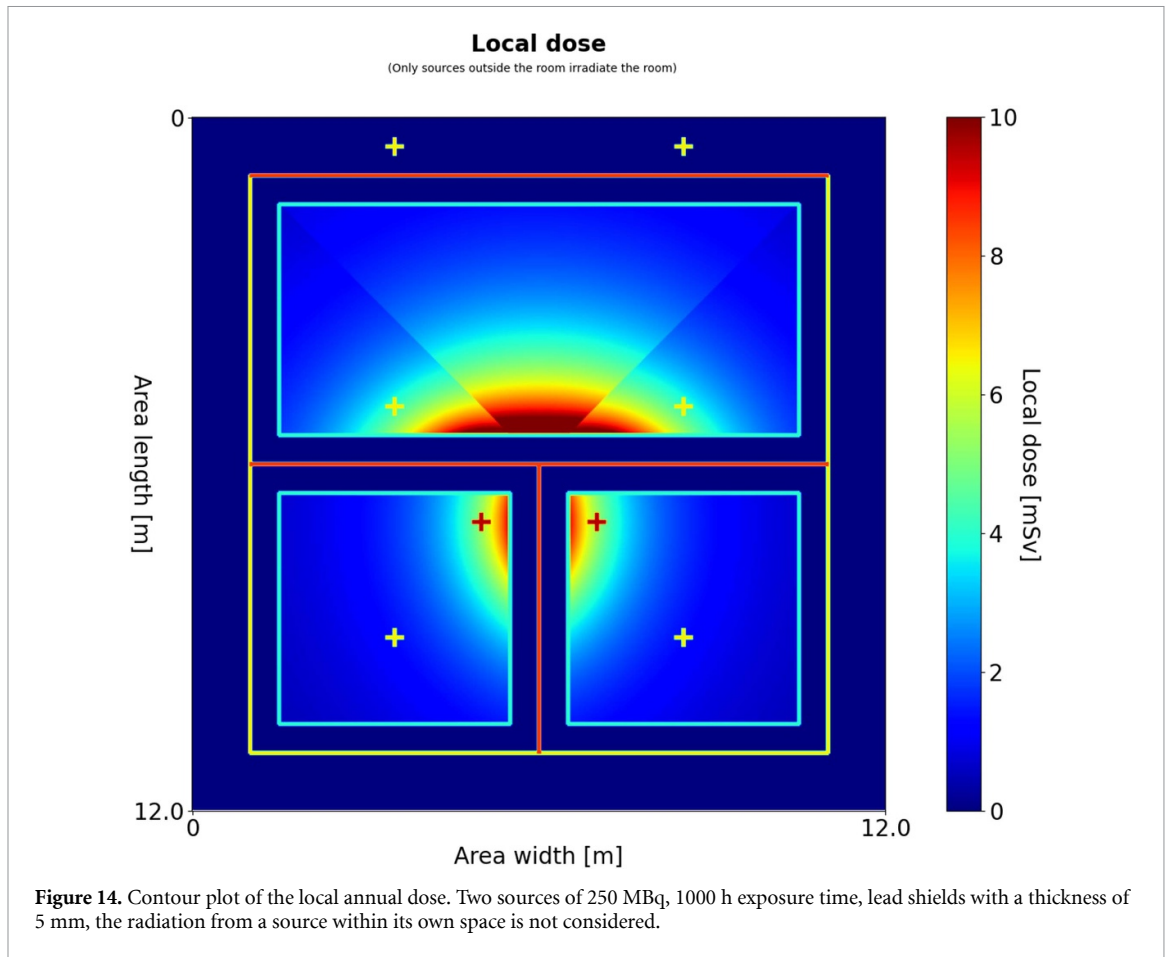
Omitting the dose from a source in the room where it is placed enables the planning of the structural radiation protection with the aid of the contour diagrams. In general, figure 13 is not applicable to calculate the dimensions of the shield between rooms B and C because the relevant local annual dose from source S2 in room B is superimposed by the radiation of source S1. Vice versa, the radiation of source S1 in room C is superimposed by the radiation of source S2. Consequently, the dimension of the shields can only be investigated in the contour plots where the local annual dose of the source in the room containing the source is not considered. This results in the evaluation presented in figure 14. With this concept, only the fraction of incident radiation can be evaluated for calculating shield dimensions.

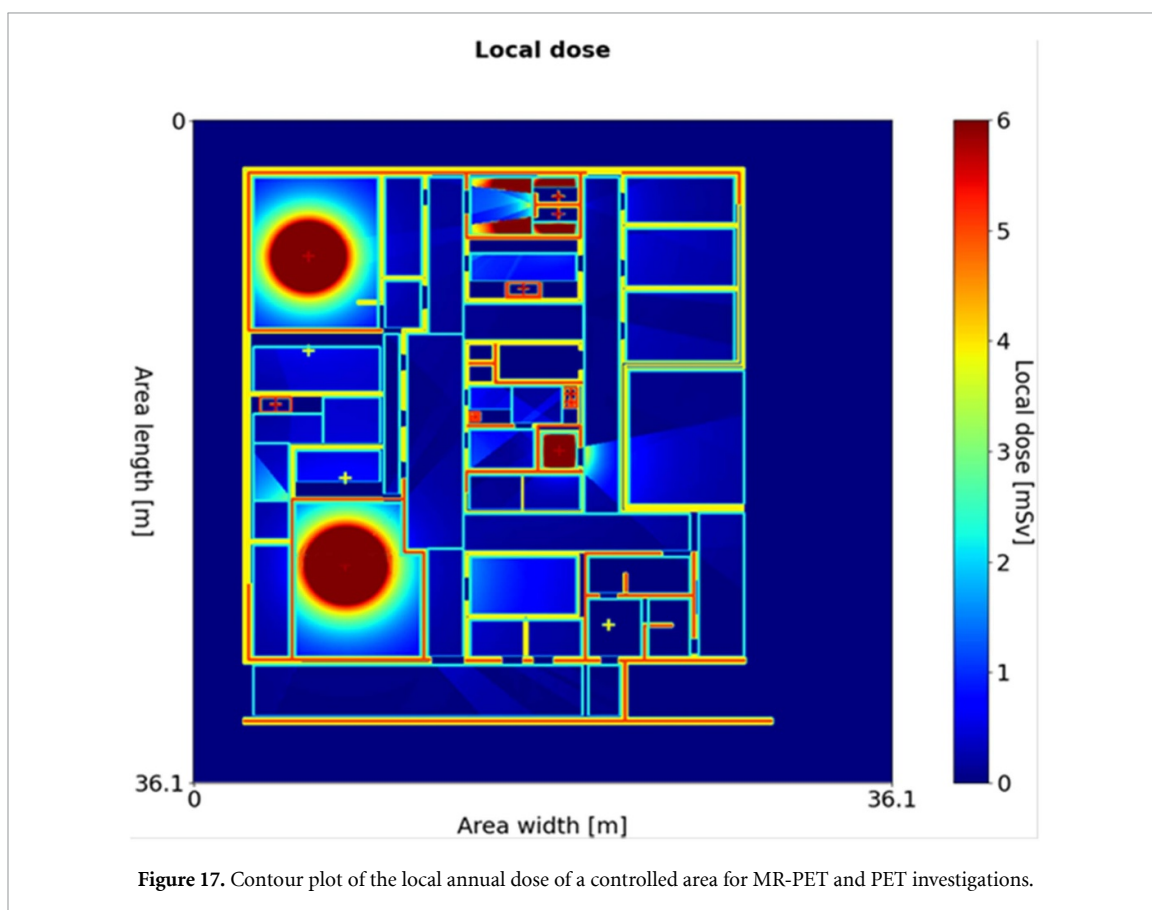
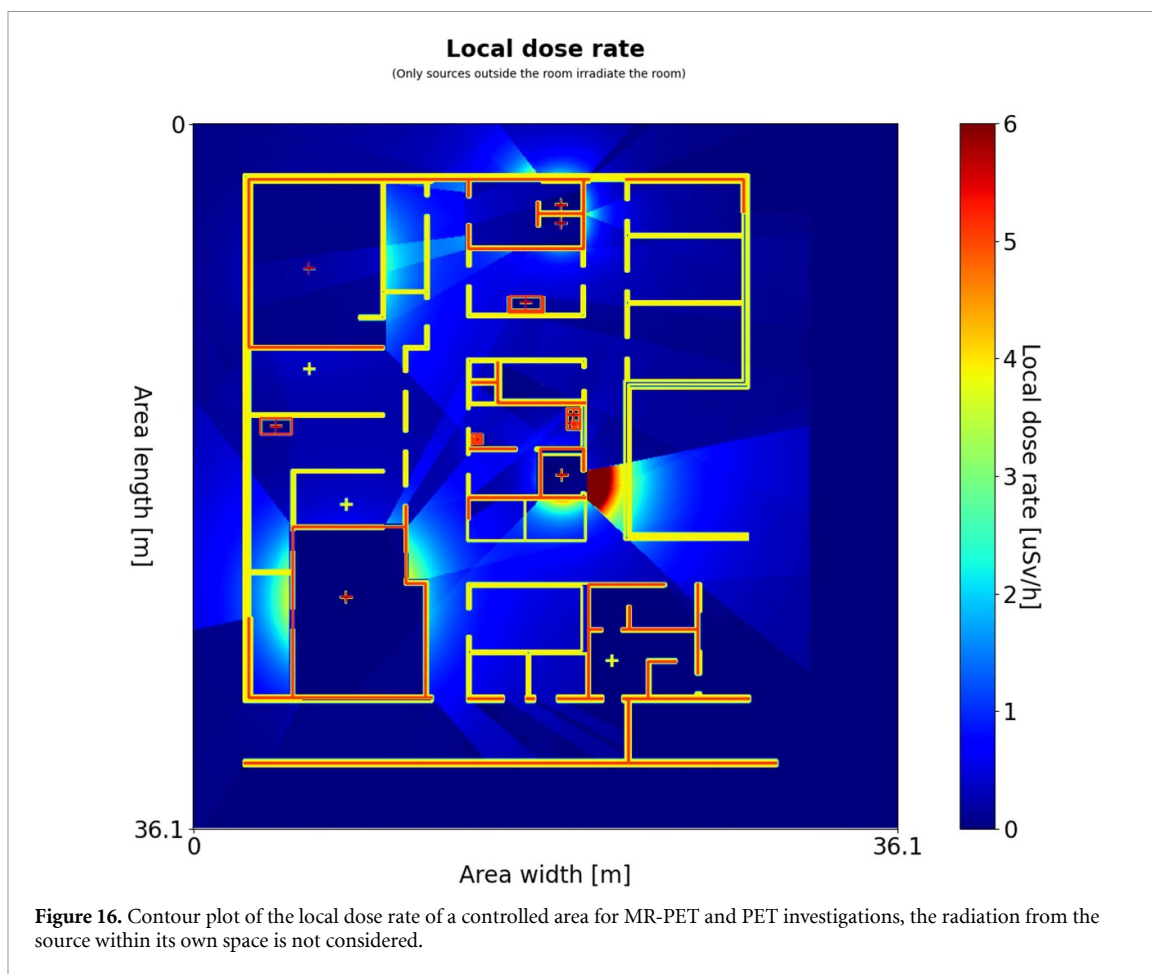
Furthermore, the contour plot can be used to assess the local dose rate within the sensitive regions of measurement equipment, such as personal contamination monitors. As the sensitive regions must not be exposed to background radiation higher than $0.2 \mu\text{Sv h}^{-1}$ [3], these areas can also be precisely planned for by using the contour plot with a lower maximal value for the local dose rate. Thus, contamination measurement devices can be placed in locations with low background radiation.

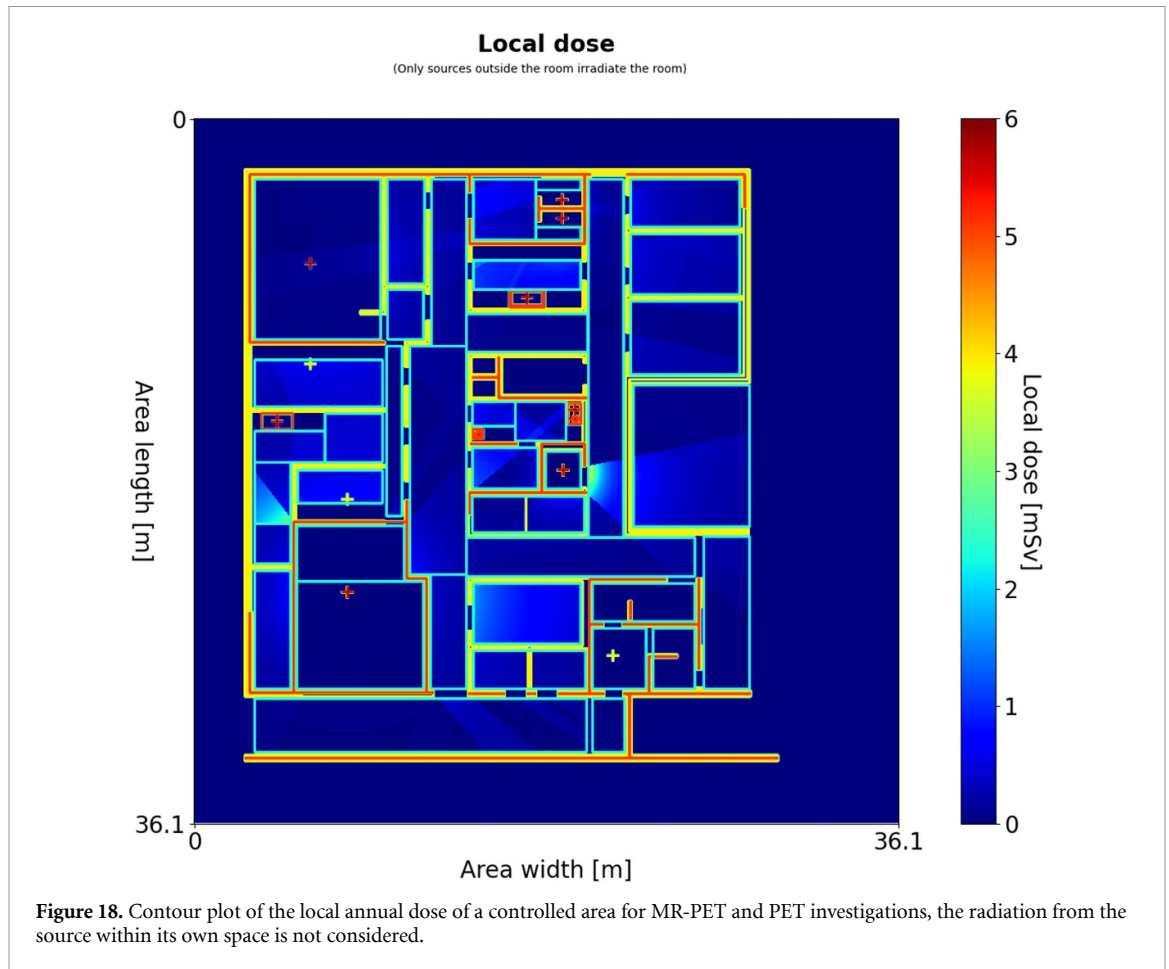
As an example, the approach is applied to a PET facility. Figure 15 shows the contour plot of the considered dose rate. Structural measures are taken within the room where sources S1 and S2 are located. In

Table 5. Verification of software output: For each marker position, the local dose rate and the local annual dose are calculated and compared with the output values of the software. First, the local dose rate is evaluated based on the radioactivity of the source and the distance between the marker and the source. Then, the absolute dose rate is calculated considering the shielding. The total dose rate is computed by superimposing the absolute dose rates of each source at the marker position. Finally, the local annual dose is calculated by the total dose rate and the exposure time.

Calculation of distance between source and marker [m]																					
Marker	Source	Source x	Source y	Marker x	Marker y	Distance	Radioactivity [GBq]	Local dose rate ($\mu\text{Sv h}^{-1}$)		Shield 1 lead (mm)		Shield 2 lead (mm)		Total attenuation factor	Absolute dose rate ($\mu\text{Sv h}^{-1}$)	Total dose rate ($\mu\text{Sv h}^{-1}$)		Exposure time (h)	Result of calculation	Output of Software	
								dose rate	Attenuation factor 1	Attenuation factor 2	Attenuation factor 1	Attenuation factor 2	Result of calculation			Output of Software					
1	1	4	6	2.5	-0.5	6.671	0.25	0.929	1.925	5.00	1.925	5.00	1.925	3.704	0.251	0.46	0.46	0	0	0	0
1	2	6	6	2.5	-0.5	7.382	0.25	0.758	1.925	5.00	1.925	5.00	1.925	3.704	0.205	0.46	0.46	0	0	0	0
2	1	4	6	7.5	-0.5	7.382	0.25	0.758	1.925	5.00	1.925	5.00	1.925	3.704	0.205	0.46	0.46	0	0	0	0
2	2	6	6	7.5	-0.5	6.671	0.25	0.929	1.925	5.00	1.925	5.00	1.925	3.704	0.251	0.46	0.46	0	0	0	0
3	1	4	6	2.5	4	2.500	0.25	6.612	1.925	5.00	1.000	1.925	1.925	3.436	3.436	4.12	4.12	1000	4.12	4.12	4.12
3	2	6	6	2.5	4	4.031	0.25	2.543	1.925	5.00	1.925	5.00	1.925	3.704	0.687	4.12	4.12	1000	4.12	4.12	4.12
4	1	4	6	7.5	4	4.031	0.25	2.543	1.925	5.00	1.925	5.00	1.925	3.704	0.687	4.12	4.12	1000	4.12	4.12	4.12
4	2	6	6	7.5	4	2.500	0.25	6.612	1.925	5.00	1.000	1.925	1.925	3.436	3.436	1.32	1.32	1000	1.32	1.32	1.32
5	1	4	6	2.5	8	4.031	0.25	2.543	1.925	5.00	1.000	1.925	1.925	3.436	3.436	1.32	1.32	1000	1.32	1.32	1.32
6	1	4	6	7.5	8	4.031	0.25	2.543	1.925	5.00	1.000	1.925	1.925	3.436	3.436	1.32	1.32	1000	1.32	1.32	1.32
6	2	6	6	7.5	8	2.500	0.25	6.612	1.925	5.00	1.000	1.925	1.925	3.436	3.436	1.32	1.32	1000	1.32	1.32	1.32







the contour plot, the radiation paths of these sources are clearly visible, and shields can be adjusted exactly to meet the radiation protection requirements inside the room of the sources. Figure 16 shows the contour plot of the dose rate where the radiation of the source inside the room in which it is located is not considered. Here, the measures in structural radiation protection are optimised, and the effect of the shields is investigated. As a preliminary result, one can see that the local dose rate is only significantly increased in front of the toilet. With the assignment of working hours and radiation times, a contour plot of the annual dose can be investigated.

Figures 17 and 18 show the results of the structural radiation protection. Due to the short duration of stay in the corridors, there is practically no relevant effect on the calculated annual dose. The increased local dose rate in the corridor in front of the toilet also appears acceptable because of the short duration of stay, rendering additional measures unnecessary. Naturally, the increased dose near the sources remains as shown in figure 17. Thus, the direct exposure to the sources is mitigated by operating procedures.

8. Conclusion

The RadSoft software package presented here offers a straightforward but effective solution for the multi-parameter modelling of sources and shields in structural radiation protection. Although the programming of a user interface and graphical assistance in the data acquisition of complex building structures has not been implemented, the visualisation of the local dose rate and the local annual dose already shows the potential for solving complex tasks in structural radiation protection. As a result, optimised structural radiation protection increases safety for the employee and, in addition, affords considerable savings in construction costs.

The software has been successfully used to plan and optimise the structural radiation protection for a radiological medical facility. The practical examples based on a PET facility show that the graphical visualisation can effectively support the development of the structural measures. Moreover, the preparation of the required documentation for the approval procedure of a controlled area is significantly supported because hotspots from the local annual dose can be identified and individually evaluated.

Acknowledgments

Open access publication funded by the Deutsche Forschungsgemeinschaft (DFG, German Research Foundation) – 491111487.

ORCID iDs

Stefan Schwan  <https://orcid.org/0000-0001-9511-1376>

Christoph Lerche  <https://orcid.org/0000-0003-2749-2108>

N Jon Shah  <https://orcid.org/0000-0002-8151-6169>

References

- [1] Hendee W R and Edwards F M 1986 ALARA and an integrated approach to radiation protection *Semin. Nucl. Med.* **16** 142–50
- [2] DIN 6844–1:2020-05 Nuklearmedizinische Betriebe—Teil 1: regeln für die Errichtung und Ausstattung von Einrichtungen zur ambulanten Anwendung von offenen radioaktiven Stoffen zur Diagnostik und Therapie
- [3] DIN 6844–3:2020-07 Nuklearmedizinische Betriebe—Teil 3: strahlenschutzberechnungen
- [4] DIN 6844–2:2020-05 Nuklearmedizinische Betriebe—Teil 2: regeln für die Errichtung und Ausstattung von Einrichtungen zur therapeutischen Anwendung von offenen radioaktiven Stoffen
- [5] Madsen M T, Anderson J A, Halama J R, Kleck J, Simpkin D J, Votaw J R, Wendt R E 3rd, Williams L E and Yester M V 2006 AAPM task group 108: PET and PET/CT shielding requirements *Med. Phys.* **33** 4–15
- [6] Peet D J, Morton R, Hussein M, Alsafi K and Spyrou N 2012 Radiation protection in fixed PET/CT facilities—design and operation *Br. J. Radiol.* **85** 643–6
- [7] Grupen C 2010 *Introduction to Radiation Protection* (Heidelberg: Springer)
- [8] Tschurlovits M, Leitner A and Daverda G 1992 Dose rate constants for new dose quantities *Radiat. Prot. Dosim.* **42** 77–82